THERMAL STRESSES IN A NONUNIFORMLY COATED CIRCULAR INCLUSION

C. K. Chao

Department of Mechanical Engineering, National Taiwan University of Science and Technology, 43 Keelung Road, Section 4, Taipei, Taiwan

Keywords: conformal mapping, alternating technique, analytical continuation

Abstract

This paper presents an analytical solution for plane thermoelasticity problems of a nonuniformly coated circular inclusion under a remote uniform heat flow. Based on the technique of conformal mapping and the method of analytical continuation in conjunction with the alternating technique, the general expressions of the temperature, displacements and stresses for three dissimilar media are derived explicitly in a series form. For a limiting case that the thickness of the interphase layer is uniform, the derived analytical solutions are reduced to those of the corresponding circularly cylindrical layered media problem. Numerical results of interfacial stresses along the interface are carried out and displayed in graphic form.

1 Introduction

Boundary value problems in an elastic medium with inclusions have received considerable attention from many researchers since those problems have applications to many different engineering structures. Of various inclusions the elliptic shape has evoked the most interest among researchers. The stress field around the elliptical cavity under uniform loading for an isotropic and homogeneous material was first provided by Muskhelishvili [1]. The interaction of a point heat source with a circular inclusion was investigated by Chao and Shen [2]. The general solutions for an anisotropic solid with an elliptical inclusion under a remote uniform heat flow was given by Chao and Shen [3] using the method of analytical continuation and Lekhnitskii [4] complex potential approach.

So far, most work on inclusion problems was restricted to the two-phase model. Ru [5] investigated the effect of interphase layers on thermal stresses within an elliptical inclusion by using the Laurent series expansion. By using the same method, an exact solution for thermal stresses in a three-phase composite cylinder subject to uniform heat flow was provided by Chao et al. [6]. By using the Peach-Koehler formula, the image force due to edge dislocations interacting with a nonuniformly coated circular inclusion was investigated by Chen [7].

2 Material and methods

2.1 Basic equations

Consider a circular inclusion surrounded by an interphase layer of nonuniform thickness, which in turn is embedded in an unbounded matrix subjected to a remote uniform heat flow (see Fig. 1a). The shear moduli of S_a, S_b and S_c are denoted by G_a, G_b and G_c, respectively and the heat conductivities of S_a, S_b and S_c are denoted by k_a, k_b and k_c, respectively . Both the inner circular interface L_1 formed by S_a and S_b, and the outer circular interface L_2 formed by S_b and S_c are assumed to be perfect, i.e. both tractions and displacements are continuous across the two interfaces. The origin of the Cartesian coordinate system is chosen to be at the center of the outer circle L_1 of unit radius. The center of the inner circle L_2 of radius $R_0 = (x_2 - x_1)/2$ lies on the x-axis. The two centers of the two circles L_1 and L_2 are set apart by the distance $\triangle = (x_1 + x_2)/2$. The components of the displacements, stresses and tractions for an isotropic body under plane deformation are expressed in terms of two stress functions $\phi(z)$ and $\psi(z)$, and a temperature function $\theta(z)$ as follows [2]:

$$2G(u_x + iu_y) = \kappa\phi(z) - z\overline{\phi'(z)} - \overline{\psi(z)} + 2G\beta\int \theta(z)dz \tag{1}$$

$$\sigma_{xx} + \sigma_{yy} = 2\left[\phi'(z) + \overline{\phi'(z)}\right] \tag{2}$$

$$\sigma_{yy} - \sigma_{xx} + 2i\sigma_{xy} = 2\left[\bar{z}\phi''(z) + \psi'(z)\right] \tag{3}$$

$$-F_y + iF_x = \phi(z) + z\overline{\phi'(z)} + \overline{\psi(z)} \tag{4}$$

where $\kappa = 3 - 4\nu$ for the plane strain deformation and $(3-\nu)/(1+\nu)$ for the plane stress deformation, ν and β are Poisson's ratio and the thermal expansion coefficients, respectively. Here the prime represents the derivative with respect to $z = x + iy$, and the overbar represents the complex conjugate.

We adopt the following conformal mapping function $m(\zeta)$ [8]

$$z = m(\zeta) = \frac{\zeta - a}{a\zeta - 1} \tag{5}$$

where $a = \dfrac{1 + x_1x_2 + \sqrt{(x_1^2 - 1)(x_2^2 - 1)}}{x_1 + x_2} > 1$

The mapped ζ-plane is shown in Fig. 1b. It can be observed that the unbounded matrix S_c is mapped onto a unit disk $|\zeta| < 1$ in the ζ-plane and the point at infinity z=∞ is mapped onto $\zeta = 1/a$ in the ζ-plane, the interphase layer S_b formed by two eccentric circles L_1 and L_2 is mapped onto the annulus $1 < |\zeta| < R$ ($R = (1 - x_1x_2 + \sqrt{(x_1^2 - 1)(x_2^2 - 1)})/(x_2 - x_1) > 1$) in the ζ-plane. For convenience of calculation, we write $\phi(\zeta) = \phi(m(\zeta))$ and $\psi(\zeta) = \psi(m(\zeta))$ so that in the mapped $\zeta -$plane, the displacements, stresses and resultant forces take the form

$$2G(u_x + iu_y) = \kappa\phi(\zeta) - \frac{m(\zeta)}{\overline{m'(\zeta)}}\overline{\phi'(\zeta)} - \overline{\psi(\zeta)} + 2G\beta\int \theta(\zeta)m'(\zeta)d\zeta \tag{6}$$

$$\sigma_{xx} + \sigma_{yy} = 2\left\{\frac{\phi'(\zeta)}{m'(\zeta)} + \frac{\overline{\phi'(\zeta)}}{\overline{m'(\zeta)}}\right\} \tag{7}$$

$$\sigma_{yy} - \sigma_{xx} + 2i\sigma_{xy} = 2\left[\frac{\overline{m(\zeta)}}{m'(\zeta)}\frac{d}{d\zeta}\left\{\frac{\phi'(\zeta)}{m'(\zeta)}\right\} + \frac{\psi'(\zeta)}{m'(\zeta)}\right] \tag{8}$$

$$-F_y + iF_x = \phi(\zeta) + \frac{m(\zeta)}{\overline{m'(\zeta)}}\overline{\phi'(\zeta)} + \overline{\psi(\zeta)} \tag{9}$$

2.2 Temperature fields

For a two-dimensional heat conduction problem, the temperature function satisfies a harmonic equation. In the present study, the resultant heat flow h and the temperature T are expressed in terms of a single complex potential $\theta(\zeta)$ as [2]

$$h = \int (q_x dy - q_y dx) = -k \ \mathrm{Im}[\theta(\zeta)] \tag{10}$$

$$T = \mathrm{Re}[\theta(\zeta)] \tag{11}$$

where Re and Im denote the real part and imaginary part of the bracketed expression, respectively. The quantities q_x, q_y in Eq. (2) are the components of heat flux in x and y direction, respectively, and k stands for the heat conductivity.

The complex function for a remote uniform heat flow with the temperature gradient $\tau = -q/k$ directed at an angle λ with respect to the positive x- axis in a homogeneous infinite plane can be trivially given as

$$\theta_0(\zeta) = \tau e^{-i\lambda} z = \frac{\tau e^{-i\lambda}(\zeta - a)}{a\zeta - 1} \tag{12}$$

The alternating technique and the analytical continuation method are applied to derive the unknown stress functions in terms of $\theta_0(\zeta)$ as follows

$$\theta(\zeta) = \begin{cases} U_{ab}U_{bc}\sum_{n=1}^{\infty}(V_{cb}V_{ab})^{n-1}\theta_0\left[R^{2(n-1)}\zeta\right] & z \in S_a \\ U_{bc}\sum_{n=1}^{\infty}(V_{cb}V_{ab})^{n-1}\theta_0\left[R^{2(n-1)}\zeta\right] + V_{ab}U_{bc}\sum_{n=1}^{\infty}(V_{cb}V_{ab})^{n-1}\overline{\theta_0}(\frac{R^{2n}}{\zeta}) & z \in S_b \\ \theta_0(\zeta) + V_{bc}\overline{\theta_0}(\frac{1}{\zeta}) + U_{cb}V_{ab}U_{bc}\sum_{n=1}^{\infty}(V_{cb}V_{ab})^{n-1}\overline{\theta_0}(\frac{R^{2n}}{\zeta}) & z \in S_c \end{cases} \tag{13}$$

Integration of Eq. (13) with z yields

$$g(\zeta) = \begin{cases} \left[\frac{U_{ab}U_{bc}\tau e^{-i\lambda}(a^2-1)^2}{2a^2(a\zeta-1)^2} - \frac{U_{ab}U_{bc}\tau e^{-i\lambda}(a^2-1)}{a^2(a\zeta-1)}\right] \\ +\frac{U_{ab}U_{bc}\tau e^{-i\lambda}(a^2-1)}{a^2}\left[\sum_{n=1}^{\infty}\frac{(V_{cb}V_{ab})^n(a^2-R^{2n})}{(R^{2n}-1)(a\zeta-1)} - \sum_{n=1}^{\infty}\frac{(V_{cb}V_{ab})^n(a^2-1)R^{2n}}{(R^{2n}-1)^2}\log(\frac{aR^{2n}\zeta-1}{a\zeta-1})\right] & \zeta \in S_a \\ \left[\frac{U_{bc}\tau e^{-i\lambda}(a^2-1)^2}{2a^2(a\zeta-1)^2} - \frac{U_{bc}\tau e^{-i\lambda}(a^2-1)}{a^2(a\zeta-1)}\right] \\ +\frac{U_{bc}\tau e^{-i\lambda}(a^2-1)}{a^2}\left[\sum_{n=1}^{\infty}\frac{(V_{cb}V_{ab})^n(a^2-R^{2n})}{(R^{2n}-1)(a\zeta-1)} - \sum_{n=1}^{\infty}\frac{(V_{cb}V_{ab})^n(a^2-1)R^{2n}}{(R^{2n}-1)^2}\log(\frac{aR^{2n}\zeta-1}{a\zeta-1})\right] \\ +V_{ab}U_{bc}\tau e^{i\lambda}\left[\sum_{n=1}^{\infty}\frac{(V_{cb}V_{ab})^{n-1}(1-R^{2n})(a^2-1)}{(a^2R^{2n}-1)(a\zeta-1)} - \sum_{n=1}^{\infty}\frac{(V_{cb}V_{ab})^{n-1}R^{2n}(a^2-1)^2\log(a\zeta-1)}{(a^2R^{2n}-1)^2}\right] \\ +V_{ab}U_{bc}\tau e^{i\lambda}\sum_{n=1}^{\infty}\frac{(V_{cb}V_{ab})^{n-1}R^{2n}(a^2-1)^2\log(\zeta-aR^{2n})}{(a^2R^{2n}-1)^2} & \zeta \in S_b \\ \left[\frac{\tau e^{-i\lambda}(a^2-1)^2}{2a^2(a\zeta-1)^2} - \frac{\tau e^{-i\lambda}(a^2-1)}{a^2(a\zeta-1)}\right] + V_{bc}\tau e^{i\lambda}\log(\zeta-a) - V_{bc}\tau e^{i\lambda}\log(a\zeta-1) \\ +U_{cb}V_{ab}U_{bc}\tau e^{i\lambda}\sum_{n=1}^{\infty}\left[\frac{(V_{cb}V_{ab})^{n-1}(1-R^{2n})(a^2-1)}{(a^2R^{2n}-1)(a\zeta-1)}\right] \\ -U_{cb}V_{ab}U_{bc}\tau e^{i\lambda}\sum_{n=1}^{\infty}\left[\frac{(V_{cb}V_{ab})^{n-1}R^{2n}(a^2-1)^2}{(a^2R^{2n}-1)^2}\log(a\zeta-1)\right] \\ +U_{cb}V_{ab}U_{bc}\tau e^{i\lambda}\sum_{n=1}^{\infty}\left[\frac{(V_{cb}V_{ab})^{n-1}R^{2n}(a^2-1)^2}{(a^2R^{2n}-1)^2}\log(\zeta-aR^{2n})\right] & \zeta \in S_c \end{cases} \tag{14}$$

2.3 Stress fields

For a region bounded by a circle, say $c=|\zeta|$, we introduce an auxiliary stress function $\omega(\zeta)$ such that [5]

$$\omega(\zeta)=\frac{\overline{m}(\frac{c^2}{\zeta})}{m^{'}(\zeta)}\phi^{'}(\zeta)+\psi(\zeta) \tag{15}$$

It should be noted that unlike the standard Muskhelishvili complex functions $\phi(\zeta)$ and $\psi(\zeta)$, the function $\omega(\zeta)$ is dependent on the radius of the circular interface.

By the same method as in the previous steps, we can find all the unknown functions $\phi_n(\zeta)$, $\phi_{an}(\zeta)$, $\phi_{bn}(\zeta)$ and $\phi_{cn}(\zeta)$ (n=1,2,3…) which can be expressed in terms of $\phi_0(\zeta)$ and $\omega_0(\zeta)$ as

$$\phi(\zeta)=\begin{cases} \phi_{aa}(\zeta)+(1+\Lambda_{ab})\sum_{n=1}^{\infty}\phi_n(\zeta)-\frac{(1+\Lambda_{ab})\Pi_{ba}}{1-\Pi_{ba}^2}\left[\sum_{n=1}^{\infty}C_n^*+\Pi_{ba}\sum_{n=1}^{\infty}\overline{C_n^*}\right]h(\zeta) & \zeta\in S_a \\ M\log\zeta+\phi_{ba}(\zeta)+\phi_0(\zeta)+\sum_{n=1}^{\infty}\phi_n(\zeta)+\Lambda_{cb}^{-1}\left[\sum_{n=1}^{\infty}\overline{\omega_{n+1}}(\frac{1}{\zeta})+u(\zeta)\sum_{n=1}^{\infty}C_{n+1}\right] & \zeta\in S_b \\ N\log\zeta+\phi_{cc}(\zeta)+(1+\Lambda_{cb})\phi_0(\zeta)+(1+\Lambda_{cb}^{-1})\left[\sum_{n=1}^{\infty}\overline{\omega_{n+1}}(\frac{1}{\zeta})+u(\zeta)\sum_{n=1}^{\infty}C_{n+1}\right] & \zeta\in S_c \end{cases} \tag{16}$$

$$\omega(\zeta)=\begin{cases} \omega_{aa}(\zeta)+(1+\Pi_{ab})\sum_{n=1}^{\infty}\left[\omega_n(\zeta)+t_{21}(\zeta)\phi_n^{'}(\zeta)\right] & \\ -\frac{\Lambda_{ab}-\Pi_{ab}+\Pi_{ba}^2(1+\Pi_{ab})}{1-\Pi_{ba}^2}\overline{h}(\frac{R^2}{\zeta})\sum_{n=1}^{\infty}\overline{C_n^*}-\frac{\Pi_{ba}(1+\Lambda_{ab})}{1-\Pi_{ba}^2}\overline{h}(\frac{R^2}{\zeta})\sum_{n=1}^{\infty}C_n^* & \zeta\in S_a \\ \overline{M}\log\zeta+\omega_{ba}(\zeta)+\omega_0(\zeta)+\sum_{n=1}^{\infty}\omega_n(\zeta)+\Pi_{cb}^{-1}\sum_{n=1}^{\infty}\overline{\phi_{n+1}}(\frac{1}{\zeta}) & \\ +t_{12}(\zeta)\Lambda_{cb}^{-1}\left[\frac{1}{\zeta^2}\sum_{n=1}^{\infty}\overline{\omega_{n+1}^{'}}(\frac{1}{\zeta})-u^{'}(\zeta)\sum_{n=1}^{\infty}C_{n+1}\right]+\overline{u}(\frac{1}{\zeta})\sum_{n=1}^{\infty}\overline{C_{n+1}} & \zeta\in S_b \\ \overline{N}\log\zeta+\omega_{cc}(\zeta)+(1+\Pi_{cb})\left[\omega_0(\zeta)+t_{12}(\zeta)\phi_0^{'}(\zeta)\right] & \\ -(1+\Pi_{cb})\overline{u}(\frac{1}{\zeta})\overline{C_n}+(1+\Pi_{cb}^{-1})\sum_{n=1}^{\infty}\overline{\phi_{n+1}}(\frac{1}{\zeta}) & \zeta\in S_c \end{cases} \tag{17}$$

where $t_{12}(\zeta)=-t_{21}(\zeta)=\frac{\overline{m}(\frac{1}{\zeta})-\overline{m}(\frac{R^2}{\zeta})}{m^{'}(\zeta)}$, $u(\zeta)=\frac{(a^2-1)^2}{a^3(a\zeta-1)}$, $h(\zeta)=\frac{(a^2R^2-1)^2}{a^3(a\zeta-1)}$, $C_n=a^2\overline{\phi_n^{'}}(a)$, $C_n^*=a^2\overline{\phi_n^{'}}(R^2a)$

and the recurrence formulae for $\phi_n(\zeta)$ and $\omega_n(\zeta)$ are

$$\phi_{n+1}(\zeta)=\begin{cases} \left[\overline{\omega_0}(\frac{1}{\zeta})+\overline{t_{12}}(\frac{1}{\zeta})\overline{\phi_0^{'}}(\frac{1}{\zeta})\right]-\Pi_{cb}u(\zeta)C_1 & for\quad n=0 \\ \Pi_{cb}\Lambda_{ab}\phi_n(R^2\zeta)-\frac{\Pi_{cb}\Pi_{ba}(1+\Lambda_{ab})\overline{C_n^*}h(R^2\zeta)}{1-\Pi_{ba}}-\frac{\Pi_{cb}(\Lambda_{ab}+\Pi_{ba})C_n^*h(R^2\zeta)}{1-\Pi_{ba}} & \\ -\Pi_{cb}\Pi_{ab}R^2\zeta^2\overline{t_{12}}(\frac{1}{\zeta})\left[\omega_n^{'}(R^2\zeta)+t_{21}^{'}(R^2\zeta)\phi_n^{'}(R^2\zeta)+t_{21}(R^2\zeta)\phi_n^{''}(R^2\zeta)\right] & \\ +\Pi_{cb}\Pi_{ab}\overline{t_{12}}(\frac{1}{\zeta})\overline{h^{'}}(\frac{1}{\zeta})\overline{C_n^*}-\Pi_{cb}u(\zeta)C_{n+1} & for\quad n=1,2,3... \end{cases} \tag{18}$$

$$\omega_{n+1}(\zeta)=\begin{cases} \Lambda_{cb}\overline{\phi_0}(\frac{1}{\zeta})-\overline{u}(\frac{1}{\zeta})\overline{C_1} & for\quad n=0 \\ \Lambda_{cb}\Pi_{ab}\left[\omega_n(R^2\zeta)+t_{21}(R^2\zeta)\phi_n^{'}(R^2\zeta)+\overline{h}(\frac{1}{\zeta})\overline{C_n^*}\right]-\overline{u}(\frac{1}{\zeta})\overline{C_{n+1}} & for\quad n=1,2,3... \end{cases} \tag{19}$$

For a limiting case of interphase layer with uniform thickness, i.e., $\Delta=0$ (or $x_1=-x_2$), the above solutions, Eq. (16) and Eq. (17), reduce to an exact solution for the corresponding circular inclusion problem [5].

3 Results and discussion

The thermal potential in Eq. (13) is expressed in terms of a homogeneous solution $\theta_0(z)$ through the non-dimensional bimaterial constants V and U . The present series solution converges to the true solution since those bimaterial constants are always less than one. The stress functions as indicated in Eqs. (16), (17) which may be calculated from $\phi_0(z)$ and $\omega_0(z)$ through the non-dimensional bimaterial constants Λ and Π . For most combinations of materials, Λ and Π are less than 1 and 0.5, respectively, which guarantees rapid convergence. Consequently, the convergence rate becomes more rapid as the differences of the elastic constants of the neighboring materials get smaller. Even though materials *a* and/or *c* are rigid or non-existent, the solution remains valid. For a limiting case of an uniformly coated inclusion problem, $\Delta = 0$ (or $x_1 = -x_2$) , the above solutions, Eq. (16) and Eq. (17), can be reduced to an exact solution . The angular variations of interfacial stresses for a three-phase cylinder are discussed in detail and shown in graphic form. Note that all the calculated results shown in fig. 2 is determined by summing up to $n = 3$ of Eq. (16) and Eq. (17) respectively, since they are checked to achieve a good accuracy with an error less than 0.59% for the current problem. Note that all the numerical results are presented for the condition that a uniform heat flow is approached from the negative x-axis. Fig. 2a show the variations of the normal interfacial stresses between material *b* and material *c* for various shear moduli ratio of a three-phase cylinder. It is clear that both the normal stress and shear stress increase with the difference of the shear moduli of the neighboring materials. It can be observed that both the interfacial normal and shear stresses are strongly dependent on the thermal expansion coefficient of the neighboring materials in figs. 2b based on the above findings, it can be concluded that the interfacial stresses of the current system can be reduced significantly if the differences of the elastic constants of the neighboring materials get smaller. Furthermore, it is evident that the maximum tensile (or compressive) stress occurs around the location having a lower (or higher) temperature.

4 Conclusion

A general analytical solution is given for the temperature and thermal stresses due to an uniform heat flow disturbed by a nonuniformly coated circular inclusion. Based on the method of analytical continuation and the alternating technique, a rapidly convergent series solution for both the temperature and thermal stresses, which is expressed in terms of the complex potential of the corresponding homogeneous problem, is obtained in an elegant form. Consequently, the present solution procedures can be further extended to the corresponding problem consisting of any number of layered medium. As a numerical illustration, the interfacial stresses are presented for various material combinations and for different eccentricities. We conclude that the interfacial stresses of the current system can be reduced significantly if the differences of the elastic constants of the neighboring materials get smaller.

References

[1] Muskhelishvili N. L. Some Basic Problems of the Mathematical Theory of Elasticity, Noordhoff, Groningen, (1953).
[2] Chao C. K., Shen M. H. On Bonded Circular Inclusion in Plane Thermoelasticity, *ASME Journal of Applied Physics*, **64**, pp. 1000-1004, (1997).
[3] Chao C. K., Shen M. H. Thermal Stresses in a Generally Anisotropic Body with an Elliptic Inclusion Subject to Uniform Heat Flow, *ASME Journal of Applied Physics*, **65**, pp. 51-58, (1998).

[4] Lekhnitskii S. G. Theory of Elasticity of an Anisotropic Elastic Body, Holden-Day, San Francisco, (1963).

[5] Ru C. Q. Effect of Interphase layers on thermal Stresses within an Elliptical Inclusion, *ASME Journal of Applied Physics*, **84**, pp. 4879-4893, (1998).

[6] Chao C. K., Chen F. M., Shen M. H. Green's Functions for a Point Heat Source in Circularly Cylindrical Layered Media, *Journal of Thermal Stresses*, **29**, pp. 809-847, (2006).

[7] Chen F. M. Edge Dislocation Interacting with a Nonuniformly Coated Circular Inclusion, *Archive of Applied Mechanics*, **81**, pp. 1117-1128, (2011).

[8] Schinzinger R., Laura P. A. A. Conformal Mapping: Methods and Applications, Elsevier, New York, (1991).

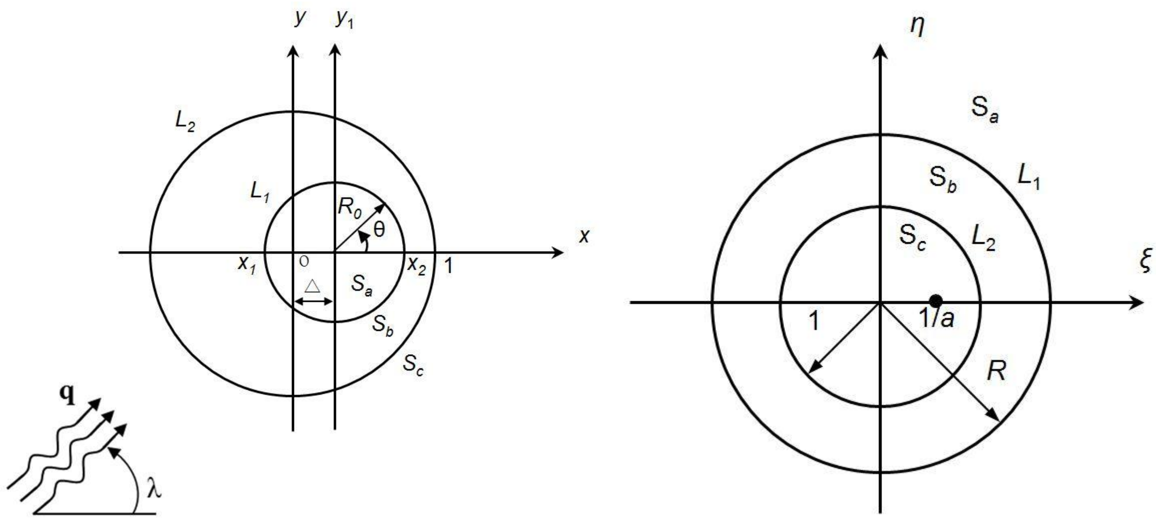

Figure 1. (a) A nonuniformly coated circular inclusion embedded in an infinite plate subjected to a remote uniform heat flow; (b) the problem in the ζ -plane

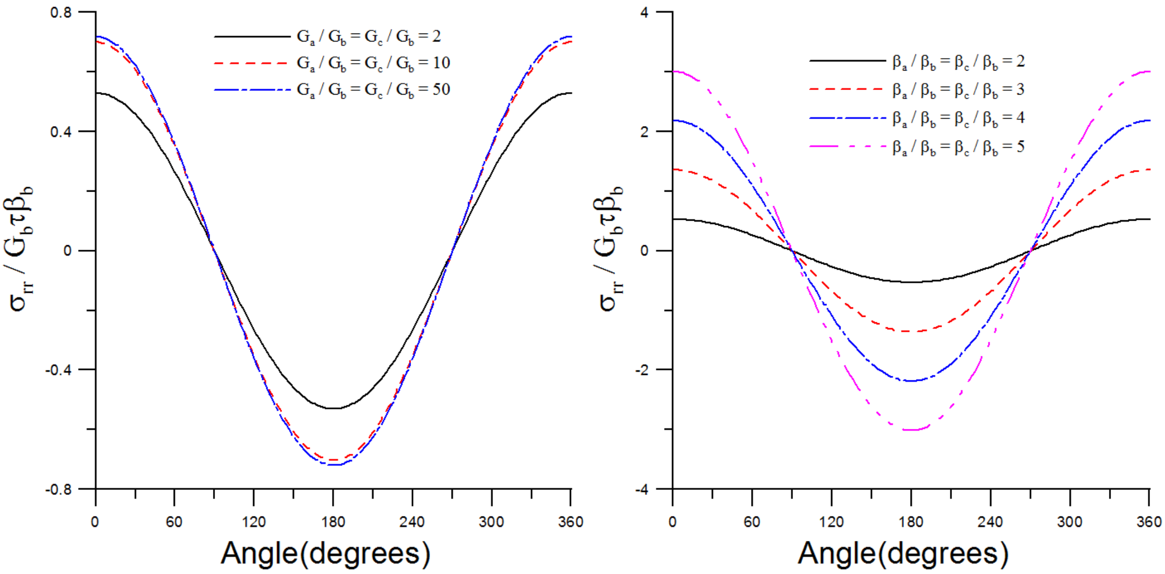

Figure 2. Angular variations of the interfacial normal stress with different ratios of (a) shear moduli (b) thermal expansion coefficients between material b and c ($\beta_a/\beta_b=\beta_c/\beta_b=2, \nu_a=\nu_a=\nu_a=0.3, \lambda=0^{\circ}, \Delta/R_0=0.0002$)